

Chimeralike states in a network of oscillators under attractive and repulsive global coupling

Arindam Mishra^{1,2}, Chittaranjan Hens^{2,4}, Mridul Bose¹, Prodyot K.Roy³, Syamal K. Dana²,

¹*Department of Physics, Jadavpur University, Kolkata 700032, India*

²*CSIR-Indian Institute of Chemical Biology, Kolkata 700032, India*

³*Department of Mathematics, Presidency University, Kolkata 700073, India and*

⁴*Department of Mathematics, Bar-Ilan University, Ramat Gan 529002, Israel*

(Dated: March 18, 2015)

We observe chimeralike states in networks of dynamical systems using a type of global coupling consisting of two components: attractive and repulsive mean-field feedback. We identify existence of two types of chimeralike states in a bistable Lienard system; in one type, both the coherent and the noncoherent populations are in chaotic states and, in the other type, the noncoherent population is in a periodic state while the coherent population is in periodic or chaotic and even be quasiperiodic. We locate the coupling parameter regimes of the two types of chimerlike states in a phase diagram. We study other bistable systems, a forced van der Pol-Duffing system and the Josephson junction model to investigate generality of the coupling configuration in creating chimeralike states. We find chaos-chaos chimeralike states in the network of bistable van der Pol-Duffing system, period-period chimeralike states in the network of Josephson junction model in the bistable regime. Furthermore, we apply the coupling to a network of chaotic Rössler system where we find the chaos-chaos chimeralike states.

PACS numbers: 05.45.Xt, 05.45.Gg

I. Introduction

Chimera states emerge [1–10] as sequentially organized subpopulations of coherent and noncoherent dynamical units due to nonlocal coupling in a network. From the first observation of this unexpected phenomenon in a network of phase oscillators [1, 2] in the weak coupling regime, till date it has been reported in limit cycle systems [7, 8] and chaotic systems [10] too. In addition to phase incoherence, amplitude incoherence of a subpopulation has also been found in the chimera states in the stronger coupling limit. Evidence of chimera states, by this time, has been supported by chemical [11], optoelectronic [12] and electronic circuit experiments [13, 14], and lately in a physical experiment [15].

Three different categories of chimera states have so far been identified [16] for nonlocal coupling. The basic chimera structure composed of a noncoherent subpopulation in a chaotic state while the coherent subpopulation could be periodic [1, 2, 4, 8, 10] or remain close to a steady state [16]. In another type of chimera states [6, 7], the noncoherent population remain in a state of spatial chaos [17] while the coherent population may be in a steady state or periodic state. A third kind of chimera states is classified as to where both the structures coexist. All three types of chimera states were reported [16] in a bistable system only for nonlocal coupling.

Chimera states are intriguing since it emerges in an ensemble of identical oscillators under symmetric coupling although nonlocal. It is more nontrivial in a population of identical oscillators under all-to-all global coupling since no spatial identity of oscillators exists. However, a population of globally coupled oscillators were reported to split [18–20] into synchronized and unsynchro-

nized subpopulations which has been preferably called as chimerlike states [19] since it is reminiscent of the chimera states although missing the spatial sequence or ordering of the oscillators. Such chimeralike states were noticed in the past [24, 26, 27], although not clearly identified, but defined very clearly, in recent time, by Sen et al [18]. Furthermore, it was observed [19] in globally coupled phase oscillators with delayed feedback, bistable systems under environmentally forced attractive and repulsive global coupling and, in limit cycle systems for a nonlinear global coupling [20]. The mechanisms of the emergence of chimeralike states differ for different coupling configurations, it is either amplitude mediated [18, 20] or amplitude modulated chimera [20] in limit cycle systems. The common feature of the chimeralike states has so far been identified as the noncoherent population belonging to chaotic states and the coherent population to periodic states. Whereas, in another type, the coherent and noncoherent populations both belong to periodic oscillations as reported [19] recently in a network of bistable systems under mixed attractive and repulsive coupling both forced into the network by an external environment.

We report here one example of bistable system, namely, a Lienard system [21] to form a globally coupled network where both the above characteristic features of coherent and incoherent populations are present in different parameter regimes of the system. We use a particular type of global coupling consisting of two components, an attractive as well as a repulsive coupling, however, like the previous example, we do not apply them as an externally forcing dynamics. The attractive coupling is a self-feedback type while the repulsive coupling may be used as a self-feedback or a cross-feedback involving other variable different from the variable where the coupling is added. Using the same coupling configuration,

we present another example of a bistable van der Pol system where we reproduce the chimeralike states, however, find only chaotic states in both the coherent and the incoherent populations. However, in a network of the superconduction Josephson junction, in a bistable regime, we observe the chimerastates where both the coherent and noncoherent populations remain in periodic states. We, particularly, provide an example of a network of chaotic Rössler system, and find evidence of the chimeralike states even when we separate the attractive and the repulsive coupling and apply them as self-feedback to two different variables.

II. Network model and Coupling configuration

The dynamics of the i th coupled unit is expressed by, $\dot{\mathbf{X}}_i = \mathbf{F}(\mathbf{X}_i, \mu) + KAB$ where $i = 1, \dots, N$; μ is the set of system parameters, K is the strength of coupling. All the dynamical units in the network are identical, $\mathbf{F} : \mathbf{R}^2 \rightarrow \mathbf{R}^2$; $\mathbf{X}_i = [x_i, y_i]^T$ where $i = 1, \dots, N$, $\mathbf{F}(\mathbf{X}_i, \mu) = [f(x_i, y_i, \mu_1, \dots), g(x_i, y_i, \mu'_1, \dots)]^T$. A is a 2×2 matrix with real values and B is a 2×1 matrix defining two types of mean-field diffusions,

$$A = \begin{pmatrix} a_{11} & a_{12} \\ a_{21} & a_{22} \end{pmatrix}, B = \begin{pmatrix} \bar{x} - x_i \\ \bar{y} - y_i \end{pmatrix}$$

where $\bar{x} - x_i = \frac{1}{N} \sum_{j=1}^N (x_j - x_i)$ and $\bar{y} - y_i = \frac{1}{N} \sum_{j=1}^N (y_j - y_i)$.

Now we explain different options of our proposed coupling configuration, *Case I*: $a_{12} = a_{21} = a_{22} = 0$ and $a_{11} = 1$ describes a typical global coupling, a type of self-feedback acting on the x -variable. *Case II*: $a_{21} = \epsilon$ and $a_{22} = 1$, all others are $a_{11} = a_{12} = 0$. The global coupling now consists of two components, one self-feedback involving the x -variable and another cross-feedback involving the y -variable; they are both added only to the same x -variable of the network. Controlling ϵ from $+ve$ to $-ve$ value, the coupling interaction changes from attractive to repulsive nature. A combined effect of K and ϵ on the collective and macroscopic behavior of the whole network is to be investigated. *Case III*: $a_{11} = 1$ and $a_{22} = \epsilon$, other two elements are zero. *Case IV*: A complex coupling when all the elements in matrix A are nonzero. We focus on the *Cases I-III* and show they are robust to create different types of chimeralike states.

III. Chimeralike states in Lienard system

We start our numerical example with a Lienard system [21] that shows bistability in isolation: a steady state coexists with periodic orbits. A peculiarity of this system is its sensitivity to initial conditions, where multiple periodic orbits appear for different set of initial conditions,

however, the periodic orbits have different frequencies, a kind of non-isochronicity [22–25]. We form a network of identical units of the Lienard system using the *Case II* coupling format,

$$A = \begin{pmatrix} 0 & 0 \\ \epsilon & 1 \end{pmatrix}; B = \begin{pmatrix} \bar{x} - x_i \\ \bar{y} - y_i \end{pmatrix}$$

when the equation for the i -th oscillator in the coupled network is expressed by

$$\dot{x}_i = y_i, \quad (1)$$

$$\dot{y}_i = -\alpha x_i y_i - \beta x_i^3 - \gamma x_i + K[\bar{y} - y_i + \epsilon(\bar{x} - x_i)]. \quad (2)$$

we take $\alpha = 0.45$, A global mean-field coupling term is added to the second equation as an attractive self-feedback but, in addition, a repulsive mean-field coupling is applied as a cross-feedback from the other variable. In a phase diagram of coupling parameters K - ϵ shown in FIG.1, we locate regions of two types of chimeralike states. In a broad parameter space (magenta/light gray region), we find the chimeralike states with both the coherent and non-coherent populations in chaotic states. However, in a very small parameter space (green/gray region), the chimeralike states show up as the coherent population remaining in a periodic state while the non-coherent population stays in a state of small chaotic or periodic and even quasiperiodic state around the steady state.

To construct this phase diagram we adopt the measures

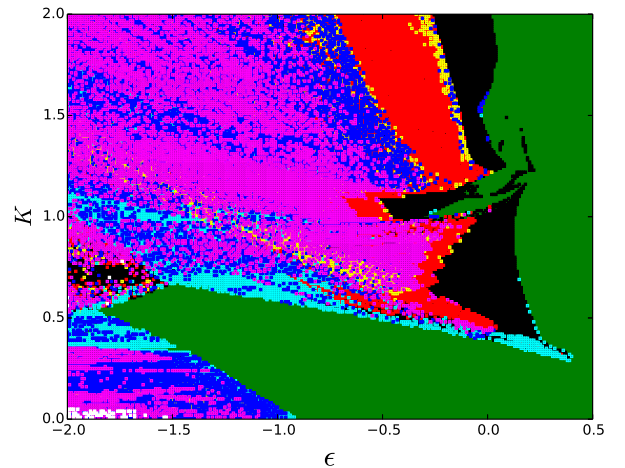


FIG. 1: $K - \epsilon$ phase space. Different colors for different states as- green: one cluster, black: two cluster, red: three cluster, yellow: four cluster, blue: chimera, magenta: multichimera, cyan: coherent state.

described in [32]. We numerically evaluate two statistical measures, namely, strength of incoherence (S) and discontinuity measure (η). The whole population is divided into M number of bins of equal length $n = N/M$ and a

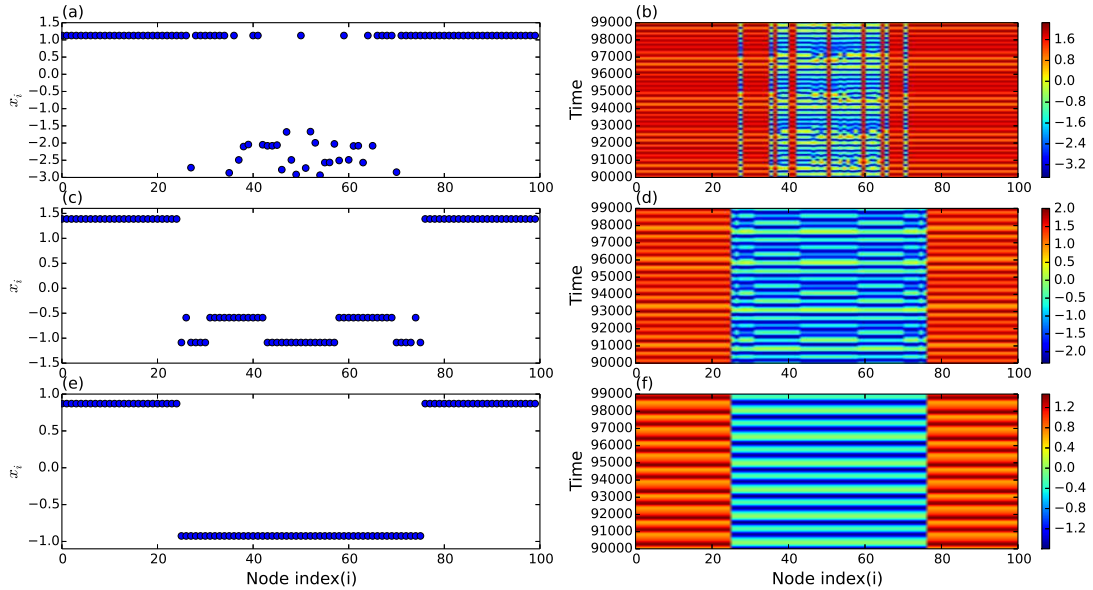


FIG. 2: Snapshots and temporal evolution for $K = 1.5$. (a) and (b) show chimera state for $\epsilon = -1.3$. (c) and (d) show three cluster for $\epsilon = -0.5$. (e) and (f) correspond to $\epsilon = -0.1$ and show two cluster state.

local standard deviation $\sigma_l(m)$ is defined as follows

$$\sigma_l(m) = \left\langle \sqrt{\frac{1}{n} \sum_{j=n(m-1)+1}^{mn} [z_{l,j} - \langle z_l^2 \rangle]} \right\rangle_t \quad (3)$$

where $m = 1, 2, \dots, M$ and $z_i = x_i - x_{i+1}$. Using this local standard deviation we measure strength of incoherence(S) as

$$S = 1 - \frac{\sum_{m=1}^M s_m}{M}, s_m = \Theta(\delta - \sigma_l(m)) \quad (4)$$

where $\Theta(\cdot)$ is the Heaviside step function, and δ is small predefined threshold.

We also calculate discontinuity measure(η), to distinguish between chimera and multichimera states, defined as

$$\eta = \frac{\sum_{i=1}^M |s_i - s_{i+1}|}{2}, (s_{M+1} = s_1) \quad (5)$$

We separate chimera, multichimera and coherent states according to (S, η) values. For chimera state: $0 < S < 1$ and $\eta = 1$. For multichimera state: $0 < S < 1$ and $2 \leq \eta \leq \frac{M}{2}$. S and η are both zero for coherent state.

We also detect different cluster states by investigating spatio-temporal evolution of the state variables of the system.

In $K - \epsilon$ phase space (FIG 1), the step sizes for K and ϵ are taken as 0.01 and we use fourth order Runge-Kutta method to integrate the system with a time step size of 0.01.

The initial states for y_i are chosen as $y_{i0} = 2(1 - \frac{4i}{N})$ for $i = 1$ to $\frac{N}{2}$ and $y_{i0} = 2(\frac{4i}{N} - 3)$ for $i = \frac{N}{2} + 1$ to N with an added small random fluctuation. All initial states for x -variables are set as zero.

There are multiple regions in the phase space. For cluster states, the region in green indicates one-cluster, whereas the black, red and yellow regions show two, three and four cluster states respectively. For chimera states, blue patches correspond to single chimera and in magenta-coloured region we find multichimera states.

In FIG.2 snapshots and temporal evolution of the x -variables are shown for chimera, two cluster and three cluster states for $K = 1.5$ and different ϵ -values. FIG.2(a) and 2(b) show chimera state for $\epsilon = -1.3$. In this chimera state both coherent and incoherent populations are chaotic in nature. FIG.2(c) and 2(d) show three cluster state for $\epsilon = -0.5$. The last row in FIG.2 corresponds to $\epsilon = -0.1$ and shows two cluster state.

FIG.3 shows another type of chimera state for $K = 0.15$ and $\epsilon = -1.6$ where oscillators from incoherent region are in periodic state and oscillators from coherent region have small chaotic oscillations around $(1, 0)$ which is the stable focus for uncoupled system. FIG.3(a) and (b) show snapshot and temporal evolution of the x -variables. FIG.3(c) is phase space diagram of an oscillator from incoherent region and 3(d) corresponds to the phase space of an os-

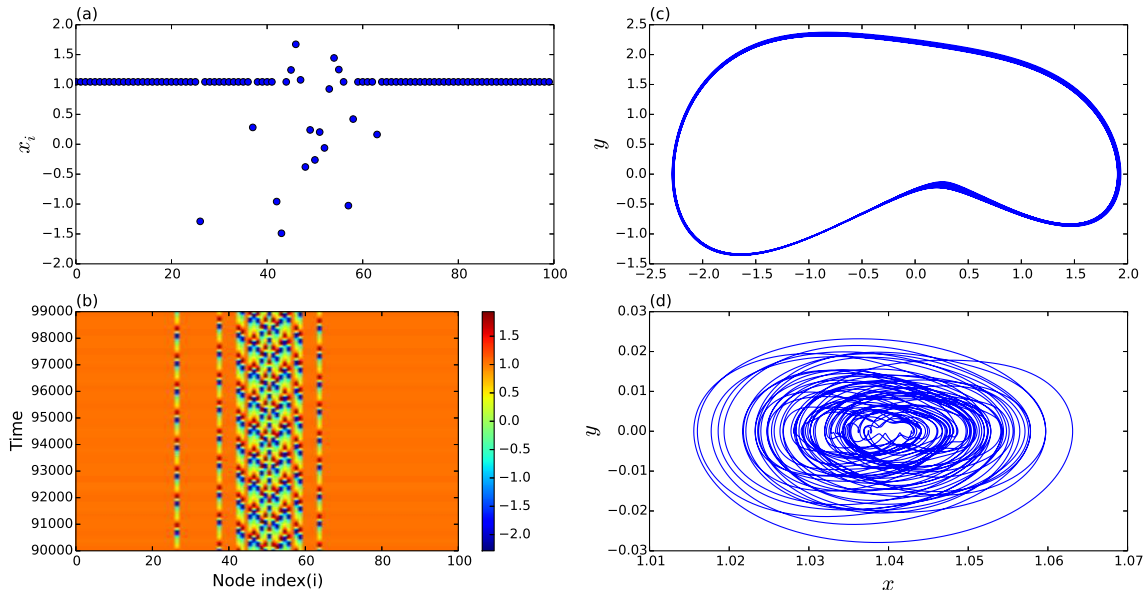


FIG. 3: Chimera state for $K = 0.15$ and $\epsilon = -1.6$. In this chimera state incoherent oscillators are periodic and coherent oscillators have small chaotic oscillations. (a) and (b) show snapshot and temporal evolution of x - variables. (c) and (d) show attractor from incoherent and coherent regions respectively.

cillator from coherent region.

IV. Chimeralike states in coupled Josephson Junction

After analyzing Lienard and forced van-der Pol-Duffing oscillators, we deploy the same coupling scheme in coupled Josephson Junction. The coupled equation for the i -th oscillator is defined as

$$\dot{\phi}_i = y_i \quad (6)$$

$$\dot{y}_i = I - \sin(\phi_i) - \alpha y_i + K[(\bar{y} - y_i) + \epsilon(\bar{x} - x_i)]. \quad (7)$$

We take parameters values as $I = 0.5$ and $\alpha = 0.2$. In this parameter space uncoupled oscillator is bistable, having one stable fixed point and a stable limit cycle.

The initial states for y_i are chosen as $y_{i0} = (2 - \frac{4i}{N})$ for $i = 1$ to $\frac{N}{2}$ and $y_{i0} = \frac{4i}{N} + 0.5$ for $i = \frac{N}{2} + 1$ to N with an added small random fluctuation. All initial states for x -variables are set as zero.

For coupling values $K = -0.17$ and $\epsilon = -0.4$, we get chimera state where both coherent and incoherent populations are in periodic state. FIG.4(a) shows snapshot of phases ϕ_i of all oscillators at a particular time and in FIG.4(b) temporal evolution of phases ϕ_i is shown.

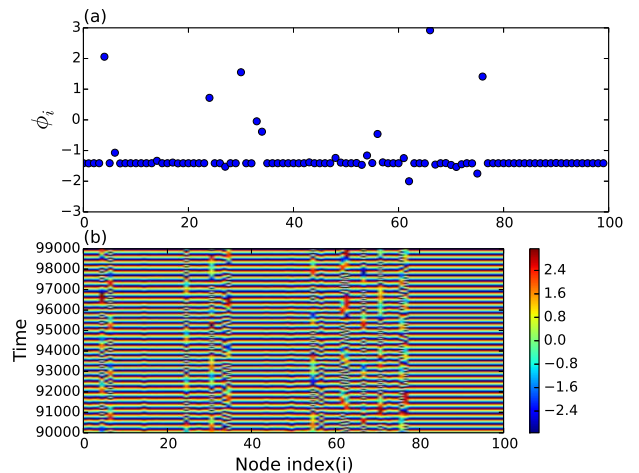


FIG. 4: Chimera state in coupled Josephson Junctions for $K = -0.17$ and $\epsilon = -0.4$. (a) shows snapshot of phases of all oscillators. (b) corresponds to temporal dynamics of phase variables.

V. Chimeralike states in forced van-der Pol-Duffing network

We construct a network of a forced van der Pol-Duffing system [16] applying the attractive self-feedback and re-

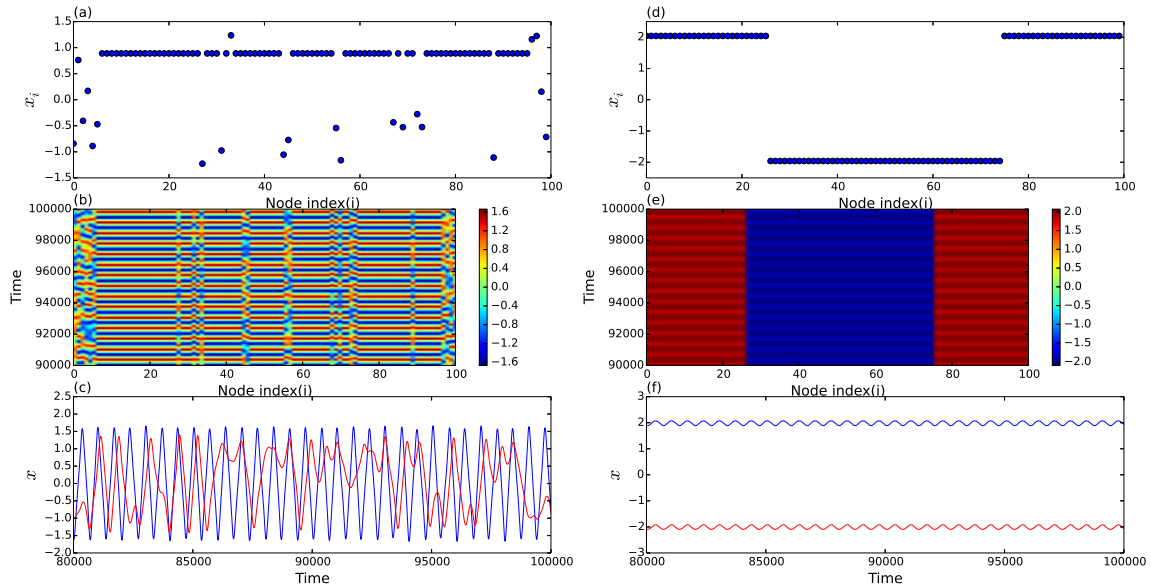


FIG. 5: Chimera and two cluster states for forced van-der Pol-Duffing oscillators for $\epsilon = -4$. (a)-(c) show chimera state at $K = 0.2$. (d)-(f) show two cluster state at $K = 1$

pulsive cross-feedback global coupling,

$$\begin{aligned} \dot{x}_i &= y_i, \\ \dot{y}_i &= \alpha(1 - x_i^2)y_i - x_i^3 + F \sin \omega t + K[(\bar{y} - y_i) + \epsilon(\bar{x} - x_i)] \end{aligned} \quad (8)$$

We take parameter values as $\alpha = 0.2$, $F = 1$ and $\omega = 0.94$. In this parameter space the oscillators are bistable, having one periodic and one chaotic attractor. The initial states for y_i are chosen as $y_{i0} = 3(1 - \frac{4i}{N})$ for $i = 1$ to $\frac{N}{2}$ and $y_{i0} = 3(\frac{4i}{N} - 3)$ for $i = \frac{N}{2} + 1$ to N and the initial states for x_i are chosen as $x_{i0} = 2(1 - \frac{4i}{N})$ for $i = 1$ to $\frac{N}{2}$ and $x_{i0} = 2(\frac{4i}{N} - 3)$ for $i = \frac{N}{2} + 1$ to N with an added small random fluctuation.

In FIG.5 we show chimera and two cluster state in forced

van-der Pol-Duffing oscillator. Left column in FIG.5 corresponds to parameter values $K = 0.2$ and $\epsilon = -4$ and shows chimera state. In this chimera state coherent oscillators are quasiperiodic and incoherent oscillators are in chaotic state. FIG.5(a) and 5(b) show snapshot of x -variables and their temporal evolution respectively. In FIG.5(c) we show the time series of x -variables of an oscillator from synchronized region (blue line) and another from desynchronized region (red line).

Right column of FIG.5 shows two cluster state for $K = 1$ and $\epsilon = -4$. FIG.5(d)-(f) show snapshot, temporal evolution and time series of x - variables. In this two cluster state oscillators from both clusters are periodic and they are completely separated in phase space.

-
- [1] Y. Kuramoto and D. Battogtokh, *Nonlin. Phen. in Complex Sys.* **5**, 380 (2002).
[2] D. M. Abrams and S. H. Strogatz, *Phys. Rev. Lett.* **93**,174102 (2004); D. M. Abrams, R. E. Mirollo, S. H. Strogatz, and D. A. Wiley, *Phys. Rev. Lett.*, **101** 084103, (2008)
[3] E. A. Martens, C. R. Laing, and S. H. Strogatz, *Phys. Rev. Lett.* **104**, 044101 (2010), S. I. Shima and Y. Kuramoto, *Phys. Rev.E* **69**, 036213 (2004).
[4] G. C. Sethia, A. Sen and F. M. Atay *Phys. Rev. Lett.* **100**, 144102 (2008).
[5] J. H. Sheeba, V. K. Chandrasekar, and M Lakshmanan, *Phys. Rev. E* **79**, 055203 (2009); **81**, 046203 (2010).
[6] I. Omelchenko, Y. L. Maistrenko, P. Hövel, and E. Schöll, *Phys. Rev. Lett.* **106**, 234102 (2011), I. Omelchenko, B. Riemenschneider, P. Hövel, Y. L. Maistrenko, and E. Schöll, *Phys. Rev. E* **85**, 026212(2012).
[7] I. Omelchenko, Oleh E. Omelchenko, P. Hövel, and Eckehard Schöll *Phys. Rev. Lett.* **110**, 224101 (2013).
[8] G. C. Sethia, A. Sen and G. L. Johnston *Phys. Rev. E* **88**, 042917 (2013).
[9] A.Zakharova, M.Kapeller, and E. Schöll, *Phys. Rev. Letts* **111**, (2014).
[10] C. Gu, G. St-Yves, and J. Davidsen, *Phys. Rev. Lett* **111**, 134101 (2013).
[11] M. R. Tinsley, S. Nkomo, and K. Showalter, *Nature Physics* **8**, 662 (2012).
[12] A. Hagerstrom, T. E. Murphy, R. Roy, P. Hövel, I. Omelchenko, and E. Schöll, *Nature Physics* **8**, 658 (2012).
[13] L. Larger, B. Penkovsky, Y. Maistrenko, *Phys. Rev.*

- Letts.*, **111**, 054103 (2013).
- [14] D.P.Rosin, D.Rontani, N.D.Haynes, E.Schöll, D.J.Gauthier *Phys. Rev. E* **90**, 030902(R) (2014).
- [15] E. A. Martens, S. Thutupallic, A.Fourrierec, and O. Halatscheka, *Proc. Natl. Acad. Sci.*, **110** (26),1056310567 (2013).
- [16] D.Dudkowski, Y.Maistrenko, T.Kapitaniak, *Phys. Rev. E.*, **90**, 032920 (2014).
- [17] L.P. Nizhnik and I. L. Nizhnik, M. Hassler, *Int. J. Bifur and Chaos* **12**, 261 (2002).
- [18] G. C. Sethia and A. Sen *Phys. Rev. Lett* **112**, 144101 (2014).
- [19] A. Yeldesbay, A. Pikovsky, M.Rosenblum, *Phys.Rev.Letts.* (2014).
- [20] L. Schmidt, K. Krischer, *Phys. Rev. Lett.* , (2014); L. Schmidt, K. Schönleber, K. Krischer, V. García-Morales, *Chaos* **24**, 013102 (2014).
- [21] V. K. Chandrasekar, M. Senthilvelan, and M. Lakshmanan, *Phys. Rev. E* **72**, 066203 (2005).
- [22] D. G. Aronson, G. B. Ermentrout, and N. Kopell, *Physica D*, **41**, 403 (1990).
- [23] E. Montbrió, B.Blasius *Chaos* **291**(2003); S.K.Dana, B.Blasius, J.Kurths, *Chaos* (2006).
- [24] H. Daido, K. Nakanishi *Phys. Rev. Lett.* **96**, 054101 (2006).
- [25]
- [26]
- [27] K. Kaneko, *Physica D* **41**, 137 (1990).
- [28]
- [29] B. van der Pol, J. Van der Mark, *Nature* **120**, 363 (1927).
- [30] F. Sorrentino, *New J. Phys.*, **14**, 033035 (2012).
- [31] S. Bilal, R.Ramaswamy, *Phys.Rev.E* **89**, 062923 (2014).
- [32] R.Gopal, V.K.Chandrasekar, A.Venkatesan, M Lakshmanan, *Phys.Rev.E* **89**, 052914 (2014).